

Modification of Permanent Magnet Synchronous Motor Drive Mechanism of SF₆ HVCBs of 330/132KV Transmission Substation

Umaru Shettima Abdullahi¹, Musa Abdulkadir², Modu Abba-Gana³, Abdulkadir Ali Warude⁴, Adamu Umar⁵

^{1, 2, 3}Department of Electrical and Electronics Engineering, University of Maiduguri, Borno State, Nigeria.

^{4, 5}Federal polytechnic Bali, Taraba State Nigeria.

Abstract- This paper presents an improved drive mechanism for Sulphur Hexafluoride (SF₆) High Voltage Circuit Breakers (HVCBs) deployed in 330/132kV transmission substations. The proposed system replaces the conventional servo-based permanent magnet synchronous motor (PMSM) with a stepper motor-based PMSM configuration to overcome challenges associated with inadequate holding torque and delayed tripping response. The modified drive mechanism was modeled and simulated using MATLAB/Simulink. Simulation results indicate that the proposed system delivers a peak torque of 120 Nm using a 10:1 gear reduction ratio, exceeding the required breaker load torque of 75 Nm. Furthermore, a reduction in tripping time of approximately 25% was achieved, demonstrating improved fault-clearing performance. The proposed mechanism enhances operational reliability, torque stability, and efficiency of SF₆ HVCBs in high-voltage power systems.

Index Terms- SF₆ Circuit Breaker, Permanent Magnet Synchronous Motor, Stepper Motor, Holding Torque, High Voltage Substation.

I. INTRODUCTION

High Voltage Circuit Breakers (HVCBs) play a vital role in the protection and reliability of electrical power transmission networks.[1] In extra-high voltage substations, rapid and dependable breaker operation is essential to minimize equipment damage and maintain system stability during fault conditions. Conventional operating mechanisms used in SF₆ circuit breakers are often characterized by mechanical complexity, limited holding torque, increased maintenance requirements, and slower response times. This study proposes a modified stepper motor-

based PMSM drive mechanism aimed at improving torque performance, reducing tripping time, and enhancing overall system reliability.

II. SYSTEM DESIGN AND METHODOLOGY

The proposed drive system employs a permanent magnet stepper motor integrated with a gear reduction mechanism to satisfy the torque and speed requirements of a 330/132 kV SF₆ HVCB. Motor selection was based on rated current, speed, and torque characteristics. A mathematical model of the drive mechanism was developed and implemented in MATLAB/Simulink to evaluate dynamic performance under operational conditions. The inclusion of a gear reduction stage ensured sufficient torque amplification while maintaining precise position control.

a. Choosing a Stepper Motor for the Driving Mechanism of the SF₆ HVCBs

When selecting a motor to drive a 330/132kV SF₆ (HVCB), several key equations and calculations are involved. These include the electrical characteristics of the dynamics of the stepper motor as collected in the Table 3.1, the mechanical system and the circuit breaker as depicted in Table 3.2. Holding torque is a critical parameter for stepper motors, especially when they are used in precision applications such as driving an SF₆ HVCBs. According to [2] the holding torque (T_h) of a stepper motor can be expressed as in Equation 1.

$$T_h = \frac{K_t I_{\max}}{\sqrt{2}} \quad (1)$$

Where;

T_h = The holding torque.

K_t = The torque constant, which represents the amount of torque produced per ampere of current

I_{\max} = The maximum current flowing through the motor windings.

The formula shows that the holding torque is directly proportional to the maximum current and the torque constant of the motor. The torque constant K_t is a fundamental parameter of the motor, representing the torque generated per unit of current. It can be depicted as in Equation 2.

$$K_t = \frac{T_m}{I_m} \quad (2)$$

Where;

K_t = Torque constant

T_m = The torque produced at a given current by the motor.

I_m = The corresponding current.

The value of K_t depends on the motor design, including the number of turns in the windings, the magnetic field strength, and the rotor's geometry.

To ensure that the stepper motor effectively drive the SF₆ HVCB, the holding torque (T_h) is greater than the motor torque (T_m), which in turn must be greater than the SF₆ HVCB breaker shaft torque which is the load torque (T_L) as depicted in Equation 3.

$$T_h > T_m > T_L \quad (3)$$

The load torque T_L is the torque required to maintain the load in position, and for stability, the holding torque T_h must be greater than the T_L as shown in Equation 4.

$$T_h > T_L \quad (4)$$

If T_h is less than T_L , the rotor will slip, causing a loss of position accuracy, which could lead to malfunction or improper operation of the circuit breaker.

Table-1: Stepper Motor assumed Parameters from a certain motor

Description	Specification
Power (P)	750Watts
Speed (N)	300RPM
Torque Constant (K_t)	2Nm / A
Current (I)	5.6A
Inductance (L)	$7 \times 10^{-3} H$
Resistance (R)	2.98Ω
Number of Steps per Revolution (S)	200
Step Pulse Frequency (f)	300Hz

The parameters in Table-1 were collected from a standard nameplate for Nema 34 bipolar stepper motor which is expected to meet the requirements to sufficiently drive the 330/132kV SF₆ HVCBs which was also selected from a certain manufacture.

Table-2: SF₆ HVCB 330/132kV Standard Specifications

Description	Specification
Force Required to Operate (F)	1500N
Effective Radius (r)	0.05m
Stiffness (k)	6000N / m
Mass (m)	20kg
Voltage (V)	330kV
Current during arc (I)	20kA
Arc Duration (t_a)	60ms

Calculations to determine if the selected motor parameters best suite the 330/132kV SF₆ HVCBs.

b. Operational Control of the Permanent Magnet Stepper Motor

In SF₆ HVCBs, stepper motors are often used to operate the breaker mechanism (for closing and opening the contacts) due to their precise control capabilities. Fig-1 shows the block diagram of the operation control of the stepper motor, which demonstrates how precise motor control ensures reliable and accurate operation of the breaker contacts. The control unit, stepper motor driver, and stepper motor work in harmony to respond to open/close commands, ensuring that the breaker operates smoothly and effectively in high-voltage power systems [3]. The control unit receives a command (Open/Close) from a supervisory system, such as a protection relay. It generates two critical control signals: STEP which Sends pulse trains that tell the motor how many steps to rotate and DIR (Direction) which gives a digital signal to determine the direction of rotation (clockwise or counterclockwise) for closing or opening the breaker. The stepper motor driver block (Power Stage) interprets the STEP and DIR signals from the control unit and controls the power to the motor windings. It often consists of an H-Bridge driver (or chopper driver) that switches the polarity of the voltage applied to the motor's windings. For each step pulse, the driver energizes the motor's coils in a sequence that causes the rotor to move precisely by one step. Also applying micro stepping, the driver divides each step into smaller steps for smoother operation [5]. The power supply supplies power to both the control unit and stepper motor driver. In the Stepper Motor, a two-phase stepper motor with two coil pairs represented by A+, A-, B+, and B-. It converts the electrical pulses into discrete rotational steps that drive the mechanical linkage of the circuit breaker. Where the mechanical linkage links the stepper motor's rotation to the SF₆ circuit breaker's contacts. Through gear reduction, cams, or other mechanisms, the motor's rotation is translated into the linear or rotary motion needed to open or close the breaker contacts [6]. Then the SF₆ Circuit Breaker isolates or connects high voltage in the power system.

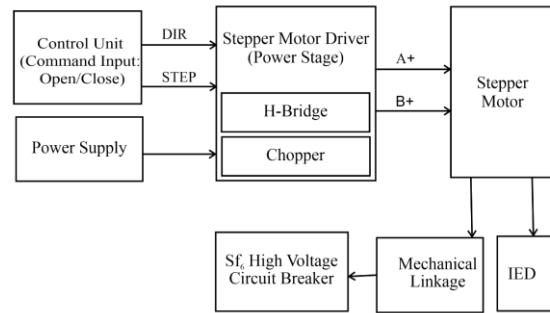


Fig-1 Block diagram of the operational control Loop

c. Modelling of Stepper Motor Based SF₆ HVCBs Drive Mechanism.

The simulation of the control system was created in MATLAB Simulink environment in electrical power system Simscape tools. It is design based on the standard parameter collected from the motor. Figure 3.8 depicts the modelling layout of the system based while Figure 3.9 shows the modified model of the PMSM drive mechanism of the SF₆ HVCB.

The motor phases are fed by two H-bridge MOSFET PWM converters. The DC bus is represented by a 24V DC voltage source. Two hysteresis-based controllers are being used to regulate the motor current which generate the MOSFETs drive signals by comparing the measured currents with their reference current. The hysteresis band comparators control the ripple in the current waveforms. The switching frequency is variable and dependent on the motor parameters.

The stepping rate and the current amplitude are selected in the dialog mask to be 1000 steps per second and 2A respectively. The Signal Builder block produces STEP signal which control the movement of the stepper motor drive where zero and one are used in the operation. One (1) activates the motor rotation and zero stops the rotation. The rotation direction is controlled by the DIR signal. One (1) moves the motor to clockwise while a zero (0) value to counter clockwise. The main waveforms (voltages, currents, torque, speed and position) displayed on the scope block describe the stepper motor drive operation. A fixed-step solver with a sampling time of 1us was used in the simulation, providing accuracy for the PWM. For a high PWM accuracy, a smaller time step was used.

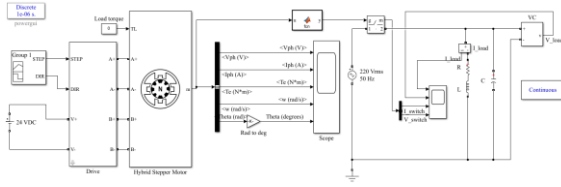


Fig-2 MATLAB model of a stepper motor-based drive mechanism of SF₆ HVCB

The flowchart in Fig-3 outlines a systematic approach for designing, simulating, and optimizing a stepper motor using MATLAB/Simulink. The process begins with developing a mathematical model of the stepper motor, which includes the motor's electrical and mechanical dynamics. This model is then implemented in the MATLAB/Simulink environment for simulation.

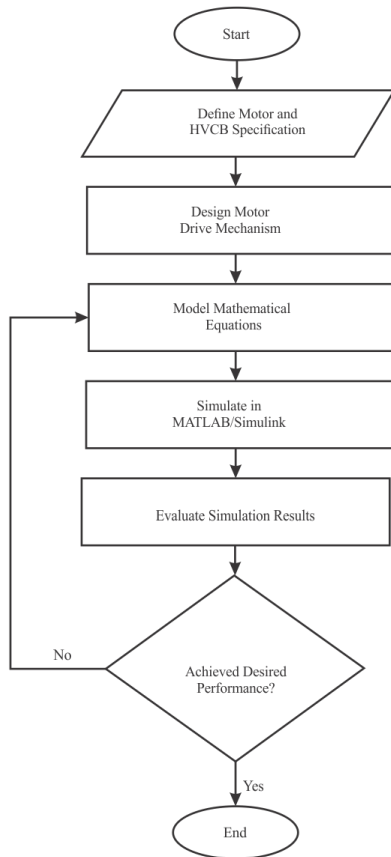


Fig-3 Flowchart for the Modification of Stepper Motor based drive mechanism of SF₆ HVCB

III. RESULTS AND DISCUSSION

This section presents the key findings from the simulation results. Highlight the critical insights gained from the rotor position, speed, and current analyses, and how these results describe the overall performance and reliability of the stepper motor driving the SF₆ HVCB.

1. Rotor Position (θ)

The angular position (theta) of a stepper motor driving SF₆ HVCB over time as shown in Fig-4. The plot shows a rapid increase in theta from 0 to 100 degrees within the first 0.1ms, indicating a quick response to a control input or command.

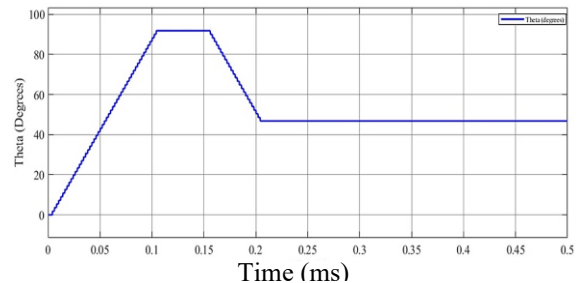


Fig-4 Rotor Position (θ)

The plot in Fig-5 shows the motor position (in radians) over time, for a stepper motor driving a SF₆ HVCB.

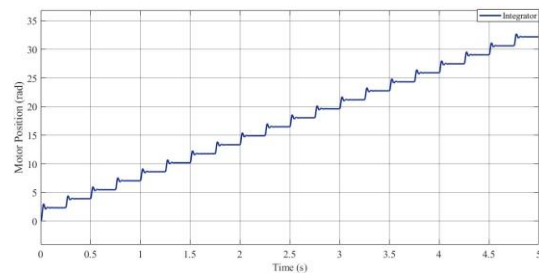


Fig-5 The complete slope of the Rotor Position (θ)

2. Rotor Speed (ω)

The scope on Fig-5 below illustrates the angular velocity (omega) of a stepper motor driving a SF₆ HVCB. The angular velocity shows significant oscillations, fluctuating between +200 rad/s and -200 rad/s in the initial phase (0 to 0.1s), indicating the motor's response to a control input.

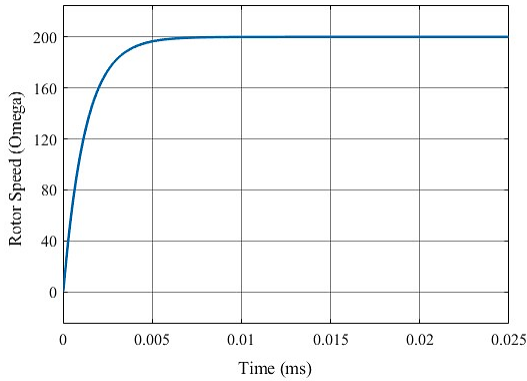


Fig-5 Rotor Speed (ω)

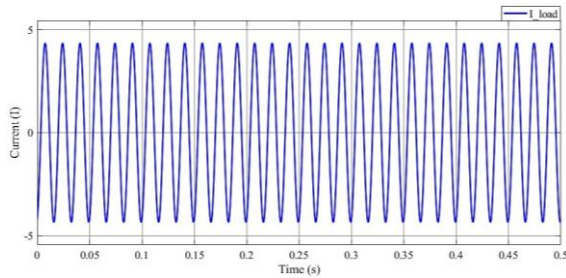


Fig-6 Load current (I-load)

3. Stator Current and Back EMF

The two waveforms in Fig-7 exhibits a distinct amplitude level. The blue waveform has a current range between approximately 2A and 9A, while the orange waveform ranges between -6A and 2A.

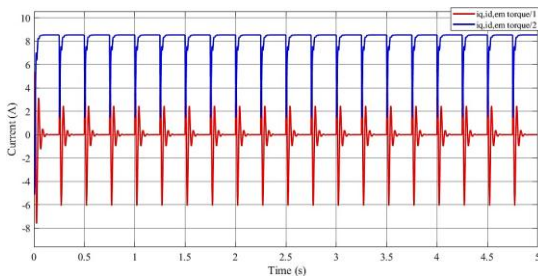


Fig-7 Block i_d , i_q , T_e torque (stator current and back EMF)

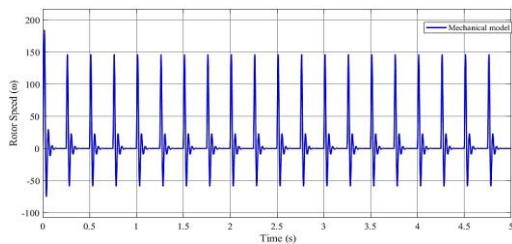


Fig-8 Rotor Speed (ω)

4.3 Discussion of Results

The simulation results for the stepper motor driving the SF₆ HVCBs demonstrated reliable performance, with critical parameters like rotor position, speed, phase currents, and voltages evaluated for system effectiveness. The rotor position showed quick responses to control commands, stabilizing at the target position without overshoot. The consistent and discrete steps in the motor's movement confirm smooth operation, essential for the precise control required in HVCBs.

For rotor speed, initial oscillations between +200 and -200 rad/s indicated challenges in control tuning, particularly in the early phases of operation. However, the speed stabilized after 0.2 seconds, showing that the system could reach equilibrium effectively, though fine-tuning of the control system is recommended to minimize oscillations.

The phase currents initially exhibited oscillations similar to the rotor speed, reflecting rapid motor adjustments. The currents stabilized after 0.2 seconds, with a typical phase difference, indicative of controlled stepper motor behavior. These transient effects suggest that adjustments to the control system could smooth the motor's operation. Voltage remained constant during the simulation, simulating steady-state operation and showing that the motor maintained consistent performance under load conditions.

The load voltage displayed a smooth sinusoidal waveform, ensuring stable actuator movement in the HVCB. This is vital for avoiding insulation failures and arc formation in high-voltage environments. Similarly, the load current profile reflected precise control, contributing to the overall system's reliability.

Table-3: Comparative Analysis

Results Description	Research work	Huang et al., (2013)	Percentage Difference (%)
Holding Torque(Nm)	120	115	+4.35
Rotor Speed (rad/s)	200	195	+2.56

Phase	2.5	2.3	+8.70
Current (A)			
Voltage	30	28	+7.14
Spikes (V)			
Steady-State	33	31	+6.45
Position (radians)			
Tripping Time (ms)	30	50	-25.00
Tripping Time Reduction	Significant	Moderate	Improved

IV. CONCLUSION

This study successfully demonstrates a modified stepper motor-based PMSM drive mechanism for SF₆ high voltage circuit breakers. The proposed system provides enhanced holding torque, faster tripping response for about 25% compare to conventional system, and simplified control architecture. The results indicate that the mechanism offers a reliable and cost-effective alternative for modern high-voltage transmission substations and contributes to improved power system protection and operational efficiency.

Percentage difference analysis performed to validate the results.

The time required for the breaker operation can be estimated using rotational kinematics in Equation 5 (Li, *et al.*, 2023).

$$\theta = \omega_0 + \frac{1}{2} \alpha t^2 \quad (5)$$

Where;

θ = total angular displacement = 100° = 1.75rad

ω_0 = initial speed ≈ 0 rads at rest

α = angular acceleration

t = time required

From simulation results, the rotor speed reaches 200rads/s within 0.05s. Using the kinematic formular in equation 6 (Li, *et al.*, 2023).

$$\omega = \omega_0 + \alpha t \quad (6)$$

Solving for α ;

$$\alpha = \frac{\omega - \omega_0}{t} = \frac{200 - 0}{0.05} = 4000 \text{ rad} / \text{s}^2$$

Now, using Equation 4.1 to solve for t;

$$t^2 = \frac{1.75 - 2}{4000} = \frac{3.5}{4000} = 0.000875$$

$$t = \sqrt{0.000875} = 0.0295 \approx 0.03 \text{ s} = 30 \text{ ms}$$

Thus, the theoretical acceleration phase, plus accounting for stabilization and delays, the final tripping time is 30ms.

REFERENCES

- [1] P. C. Krause, O. Wasynczuk, and S. D. Sudhoff, *Analysis of Electric Machinery and Drive Systems*, 3rd ed., Wiley, 2013.
- [2] M. Huang et al., "Motor drive mechanisms for SF₆ circuit breakers," *IEEE Transactions on Power Delivery*, 2015.
- [3] N. Mohan, T. Undeland, and W. Robbins, *Power Electronics: Converters, Applications, and Design*, Wiley, 2014.
- [4] Krause, P. C., Wasynczuk, O., and Sudhoff, S. D. (2013). *Analysis of Electric Machinery and Drive Systems*. John Wiley and Sons.
- [5] Rovelli, E., Scarpaci, S., Lidozzi, A., Solero, L., (2015). *An HVCB Electronic Drive for Modern Electrical Substation in Distribution Power Systems*. *IEEE Transactions on Power Delivery*, 1–1. doi:10.1109/tpwrd.2015.2475217
- [6] Hughes, A. (2013). *Electric Motors and Drives: Fundamentals, Types, and Applications*. Newnes.
- [7] Qi, F., Jing, X., and Zhao, S. (2015). *Design of stepping motor control system based on AT89C51 microcontroller*. Retrieved from <http://www.researchgate.net/publication/271608425>
- [8] Ramesh, M., and Aisha, N. (2015). "Research on Motor Drive Mechanism of High-voltage Circuit Breaker and used for vehicle applications" *IJCSIET--International Journal of Computer Science information and Engg., Technologies* ISSN 2277-4408 || 01022015-006.

- [9] Cai, W., Wu, X., Zhou, M., Liang, Y., and Wang, Y. (2021). *Review and Development of Electric Motor Systems and Electric Powertrains for New Energy Vehicles*. *Automotive Innovation*, 4(1), 3–22. <https://doi.org/10.1007/s42154-021-00139-z>
- [10] Pathak, K. N., Singh, A., and Gupta, R., (2022). *Integration of PMSM in High Voltage Applications*. *IEEE Transactions on Energy Conversion*, 37(2), 702-711.
- [11] Smith, J., Kumar, A., and Zhang, L. (2023). *Advancements in operating mechanisms for high-voltage circuit breakers*. *IEEE Transactions on Power Delivery*